Received: 04 March 2023 | Revised: 20 May 2023 | Accepted: 17 June 2023

Research Article
Journal of Research and Review in Science
56-70, Volume 10, June 2023.
DOI: 10.36108/jrrslasu/3202.01.0140

ORIGINAL RESEARCH

Seasonal Variation of the F2-Layer Critical Frequency and Comparison with the IRI-2016 Model during Two Extremes of Solar Activity Phase of Solar Cycle 22

Eugene Onori [1], Abiola Ogungbe [1] Aghogho Ogwala [2], Yusuf Kayode [1], Emmanuel Somoye[1], Razak Adeniji-Adele[1], Olorunfemi Fakunle[1]

[1]*Department of Physics, Lagos State University, Lagos, Nigeria*

[2]*Department of Physics, Eko University of Medicine and Health Sciences, Ijanikin, Lagos, Nigeria*

Correspondence
Onori Eugene O., Department of Physics, Faculty of Science, Lagos State University, Nigeria.
Email:onorieugene@gmail.com

Funding Information
This research work is self-sponsored.

Abstract:

Introduction: The variation of the ionosphere is mostly studied using the critical frequency of the F_2-layer (foF2) whose values can also be predicted by an ionospheric model. The widely used model for predicting ionospheric parameters is the International Reference Ionosphere (IRI).

Aim: This study focuses on evaluating the IRI-2016 model's performance in predicting the critical frequency of the F2-layer at equatorial stations during two extreme phases of solar cycle 22.

Methods: Experimental foF2 data from 1989 (Maximum Phase of Solar Activity) and 1986 (Minimum Phase of Solar Activity) at Ougadougou (Geomagnetic Latitude 0.59 ^{o}N, Geomagnetic Longitude 71.46 ^{o}E) in the African longitudinal sector and Manila (Geomagnetic Latitude 3.4 ^{o}N, Geomagnetic Longitude 191.1 ^{o}E) in the Asian longitudinal sector, along with IRI-2016 predictions, were analyzed and categorizing into four seasons and considering various diurnal periods of the day.

Results: The results indicate that the IRI-2016 model exhibits both overestimation and underestimation of foF2 values at different times, with more significant discrepancies during the post-midnight hours and during the equinox and solstice seasons. However, the seasonal mean values of the IRI-2016 model show improvement, closely matching observed foF2 values at the two stations.

Conclusion: The IRI-2016 model, discrepancies are more pronounced in MPSA year than MnPSA year. The URSI option excels over the CCIR option, with closer predicted values to observed values. Both options perform better in the Asian longitudinal sector compared to the African sector.

Keywords: Critical Frequency, F2-Layer, International Reference Ionosphere, Solar Activity, URSI, CCIR

All co-authors agreed to have their names listed as authors.

This is an open access article under the terms of the Creative Commons Attribution License, which permits use, distribution and any medium, provided the original work is properly cited.

1. INTRODUCTION

The F2-layer is the most conspicuous and crucial of all the ionospheric layers for radio propagation phenomena [1]. Solar radiation has a big impact on it. Low latitudes have concentration that do not drop off continuously throughout the night and even rises occasionally [2]. The F2-layer, which is present 24 hours a day in all solar-terrestrial conditions, is the most significant layer in the ionosphere. Even though the F2 layer exhibits anomalous behavior, it is still thought to be the layer that contributes the most electrons to the entire ionosphere. Ionization drift motions in the earth's magnetic field, which are principally driven by electromagnetic E x B forces, are the cause of the F2 layer's abnormal behavior (1-3).

Numerous studies on variations in the ionospheric F2 layer critical frequency (foF2) range from those that are focused on a small number of stations, a single station, or a sector, to those that looked at specific parameters over a large geographic area. These studies include [4], [5], [6], [1], [7], [8], [9], and [10] as few examples. Recent studies on the F2-layer critical frequency variability of the ionosphere and comparisons with IRI-models have been conducted. These studies differ in the specific ionospheric parameter being studied, the latitude or longitudinal sector taken into consideration, and the solar cycle dispersion of the data employed. Some of these studies include those of [11,12], [13], [14 ,15], [34], [17,18], [19, 20], [21], [22 – 24], [25], [26],[27- 29], [30].

Ionospheric models, like the International Reference Ionosphere (IRI) model, are intricate mathematical simulations of the Earth's ionosphere that seek to forecast its behavior in response to various input parameters. As new information and advances in space science become accessible, these models are regularly improved and updated. With more than 50 members from various countries, the International Union of Radio Science (URSI) and the Council on Space Research (COSPAR) collaborated to create the IRI. The IRI model, which is accessible through the IRI portal, is continually being built and improved by the IRI working team [31], [32 – 36].

During both the maximum and minimum phases of Solar Cycle 22, it would have been vital to gather comprehensive and good observational data over equatorial areas. This would require measurements of electron density, critical frequencies, scintillations, and other ionospheric features in order to facilitate detailed analysis and modeling attempts. Along with testing and improving current models using available data, developing models that can effectively depict the intricate ionospheric dynamics throughout different solar activity phases might have been the objective. In order to demonstrate how well the current International Reference Ionosphere (IRI-2016) model performs, in predicting the variation of the critical frequency of the F2-layer (foF2) over two equatorial stations during Maximum Phase of Solar Activity (MPSA) year (1989), and Minimum Phase of Solar Activity (MnPSA) year (1986) of solar cycle 22, this paper uses data from two equatorial stations [21].

2. MATERIAL AND METHODS

The data used are the mean hourly foF2 experimental data observed at Ougadougou (OUG) monthly, Geomagnetic Latitude 0.59 ^{o}N, Geomagnetic Longitude 71.46 ^{o}E in the African longitudinal sector; and Manila (MAN), Geomagnetic Latitude 3.4 ^{o}N, Geomagnetic Longitude 191.1 ^{o}E in the Asia longitudinal sector, during the MPSA year (1989) and MnPSA year (1986) respectively. The IRI-2016 model predicted foF2 data for each year. Zurich Sunspot number (Rz) data was used as index for the level of solar activity for each of the years. The observed foF2 ionosonde data and Rz data were obtained from the Space Physics Interactive Data Resource (SPIDR) website (http://spidr.ionosonde.net/) which was last accessed on the 14th of March, 2017, before the site became unavailable, while the current IRI-2016 model data used in this study were obtained from the Community Coordinated Modelling Centre (CCMC) IRI website: (https://ccmc.gsfc.nasa.gov/modelweb/models/iri2016_vitmo.php).
Analysis were carried out by first grouping the foF2 data of both observed and IRI-2016 model values into four different seasons comprising of three months each and was averaged. The seasonal mean of the IRI-

2016 modeled foF2 values were compared with the experimental or observed foF2 data. Furthermore, percentage deviation of the model from the experimental data were evaluated using equation 1.

$$\% \, Dev = \left(\frac{f_0F_{2\,Observed} - f_0F_{2\,IRI}}{f_0F_{2\,Observed}} \right) \times 100 \qquad (1)$$

This was done for the two stations for the two extreme solar phases. Thereafter, seasonal plots and plots of the percentage deviations against local time (LT) in hour (h) were plotted and discussed.

3. RESULTS AND DISCUSSION

3.1 Seasonal variation of Observed foF2 with IRI-2016 Modeled foF2 during Maximum Phase of Solar Activity (MPSA) Year

Fig. 1 – 2 (a) – (d) highlights the comparison plots between the observed foF2 and IRI - 2016 model (URSI and CCIR options) during the MPSA year (1989). The error bars on each of the observed plots in the figures indicate the respective standard deviation about the mean for each of the seasons. At the two stations, the diurnal variations of predicted f_0F_2 values of the IRI-2016 model (URSI and CCIR options) showed the same trend with those observed by ionosonde measurements. The observed response at the two stations revealed a better fit with both IRI-model options during all the seasons although the observed foF2 data were underestimated and overestimated at some time of the day and night by both options of the IRI-2016 model prediction. However, most of this overestimation and underestimation by the IRI-2016 model falls within the range of the error bar (standard deviation) of the measured data, implying very little disagreement.

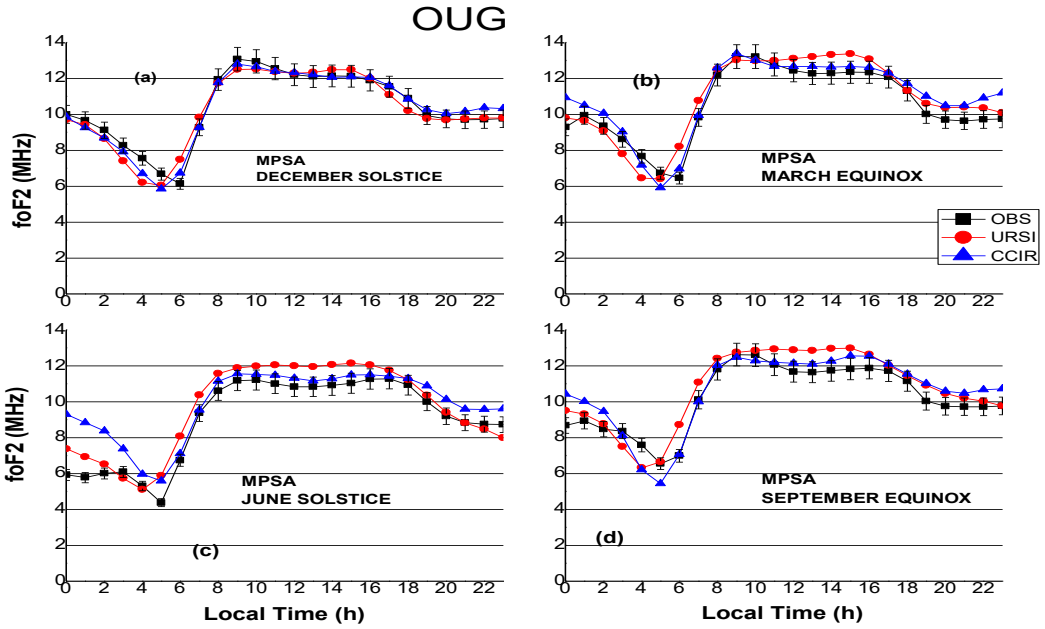

Fig. 1: Comparison plot between Observed foF2 and IRI-2016 Model (URSI and CCIR Options) for Maximum Phase of Solar Activity (MPSA) year 1989 at Ougadougou during (a) December Solstice (b) March Equinox (c) June Solstice and (d) September Equinox. The error bar in each of the plot indicates standard deviation about the mean for each of the season.

At Ougadougou (African longitudinal sector) during the MPSA year, both options of the IRI-2016 model show good agreement to a large extent with the observed foF2 during all seasons. However, both the URSI and CCIR options of the model overestimated the observed foF2 at Ougadougou between (00:00 – 05:00

LT) in June solstice and between (20:00 – 23:00 LT) in March equinox. The CCIR option overestimated the observed foF2 values between (21:00 – 23:00 LT) in June solstice, March equinox and September equinox, respectively, as seen in Fig.1 (a) – (d).

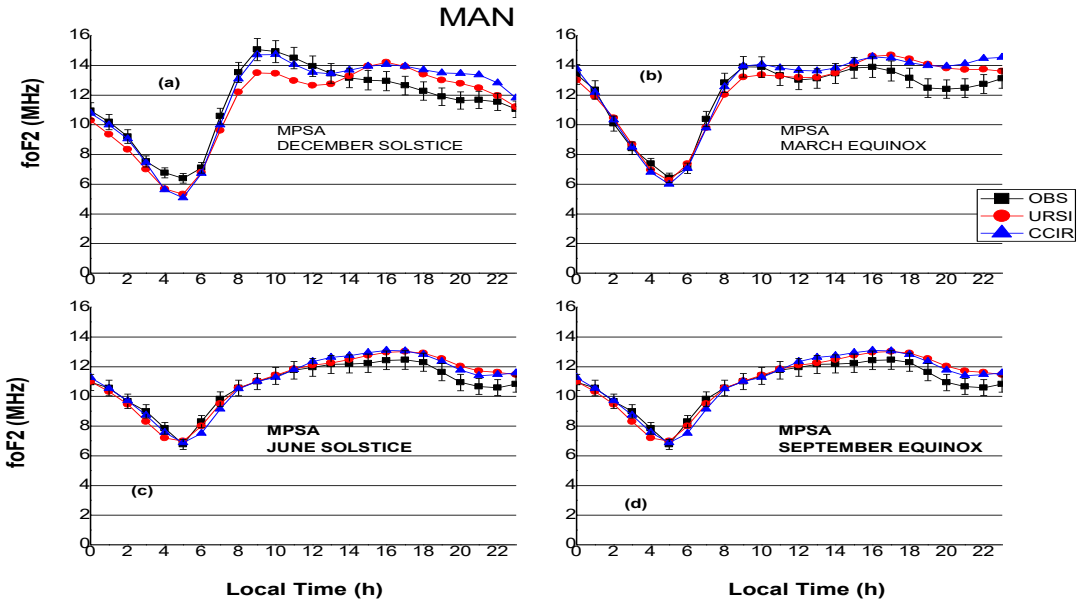

Fig. 2: Comparison plot between Observed foF2 and IRI-2016 Model (URSI and CCIR Options) for Maximum Phase of Solar Activity (MPSA) year 1989 at Manila during (a) December Solstice (b) March Equinox (c) June Solstice (d) September Equinox. The error bar in each of the plot indicates standard deviation about the mean for each of the season.

From (Fig. 2 (a) – (d), at Manila (Asian longitudinal sector), the IRI-2016 derived foF2 and observed foF2 fit reasonably well for all seasons during MPSA year with very little patches of overestimation and underestimation. Nevertheless, the IRI-2016 model overestimated the observed foF2 between (16:00 – 22:00 LT) in December solstice and March equinox respectively. [23], reported comparable observations while working with IRI-2012 model at another station, but with different sets of data.

3.2 Seasonal Variation of Observed foF2 with IRI-2016 Modeled foF2 during Minimum Phase of Solar Activity (MnPSA) Year

Fig. 3 – 4 (a) – (d) revealed the comparison plots between the observed foF2 and IRI - 2016 model (URSI and CCIR options), and the error bar on each of the observed plots in all the figures indicates as explained in section 3.1 above. Generally, at the two stations, the diurnal variation of predicted foF2 values of the IRI-2016 model with (URSI and CCIR options) show similar trend with those observed by ionosonde measurements. For the MnPSA year, the observed response at Ougadogou and Manila revealed an improved fit with the two options of the IRI-2016 model during all the seasons. Although the foF2 data were observed to have some patches of underestimation and overestimation at some time of the day and night by both options of the model. These overestimation and underestimation by the IRI-2016 model nevertheless as earlier explained, fall within the standard deviation range in the observed data, implying very little disagreement [2].

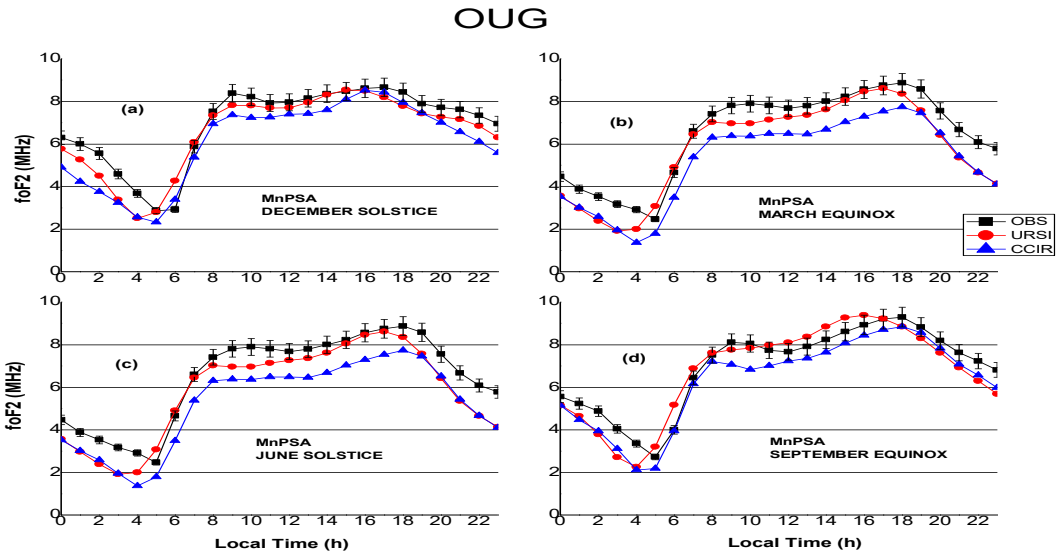

Fig. 3: Comparison plot between observed foF2 and IRI-2016 model (URSI and CCIR options) for Minimum Phase of Solar Activity (MnPSA) year 1986 at Ougadougou during (a) December Solstice, (b) March Equinox, (c) June Solstice and (d) September equinox seasons. The error bar in each of the plot indicates standard deviation about the mean for each of the season.

At Ougadougou during MnPSA year, both options of the IRI-2016 derived foF2 showed good agreement with the observed foF2 for all seasons at both stations Fig.3 (a) – (d). However, both model options underestimate the observed foF2 values between (00:00 - 00:04 LT) and (08:00 – 23:00 LT) in June solstice and March equinox.

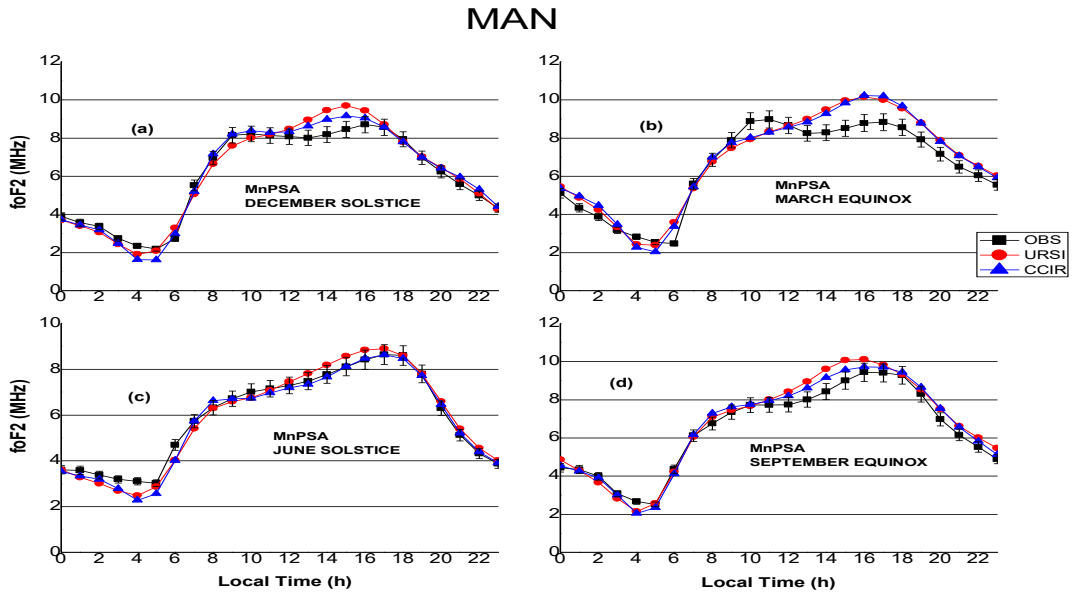

Fig. 4: Comparison plot between observed foF2 and IRI-2016 model (URSI and CCIR options) for Minimum Phase of Solar Activity (MnPSA) year 1986 at Manila during (a) December Solstice, (b) March Equinox, (c) June Solstice and (d) September equinox seasons. The error bar in each of the plot indicates standard deviation about the mean for each of the season.

While at Manila, the IRI 2016 model and observed foF2 fit well for all the seasons. However, some levels of underestimation were observed between 00:00 – 04: 00 LT and 12:00 – 16:00 LT, in December solstice, between 12:00 – 16:00 LT, 09:00 – 11:00 LT and 13:00 - 23:00 LT, in March and 13:00 - 16:00 in September equinox Fig. 4 (a) – (d).

The above discrepancies observed in Fig. 1 – 2(a) – (b) and Fig. 3 – 4(a) – (b) could be ascribed to the fact that the shapes of the electron density profile in that location are not well predicted by the IRI-2016 model option, possibly, due to lack of availability of data [37, 38]. Lack of available data may be responsible since the predictive ability of IRI model according to [11, 8] is strongly dependent on the large volume of data at that place where the forecast is made. In times and locations where there are few data sources, the predictive accuracy of IRI- model may be limited.

Observations from Figs. 1, 2, 3, and 4 (a) – (d) also revealed two characteristics peaks (pre-noon peak and post- noon peak). These two peaks are found to border about a trough at around noon called noon bite-out (NBO) profile. The NBO profile is an equatorial and low latitude ionospheric characteristics depicting electron depletion caused by fountain effect indicating the presence of equatorial electrojet strength [39 – 41], [42]. The IRI-2016 model was unable to predict this NBO profile correctly because IRI model may not be able to accurately account for the variation of an ionosphere driven by electrojet strength and also influenced by the electric field in the magnetic equator region without discrepancy [43, 26, 42].

3.3: Percentage Deviation of Iri-2016 (URSI Option) Derived Fof2 from The Observed foF2 Values

Fig. 5 – 6 (a) – (d) presents the percentage deviations of IRI – 2016 model (URSI option) foF2 from those of the observed foF2 data for all seasons at the two stations during MPSA year (1989) and MnPSA year (1986) respectively. The percentage deviations from both stations reveal pronounced positive and negative deviations between post-midnight/post-sunrise, pre-noon/post-noon and pre-midnight periods (00:00 – 08:00 LT, 10:00 – 16:00 LT and 18:00 – 23:00 LT respectively. The negative percentage deviations observed in the plots indicates higher values of IRI-2016 model than observed- foF2 values. The reverse is the case for positive percentage deviations. The deviations between 9:00 – 18:00 LT are relatively close and follow similar patterns.

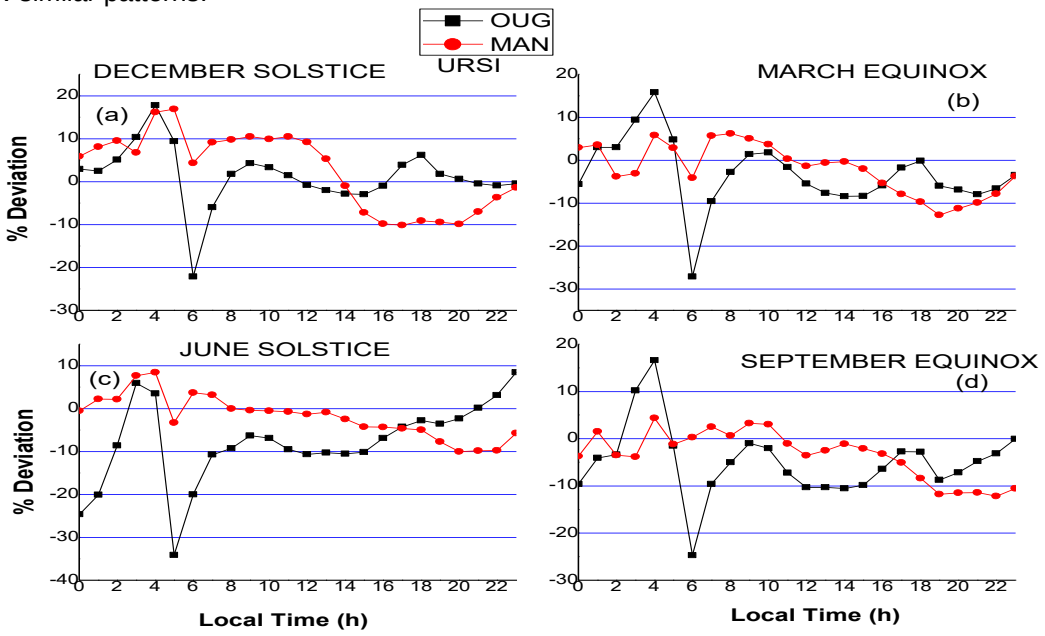

Fig. 5: Percentage deviations of the IRI-2016 (URSI option) foF2 from the observed foF2 values for all seasons across the entire stations during Maximum Phase of Solar Activity (MPSA) year, (1989)

During MPSA year, the positive and negative deviations occurring between 04:00 – 07:00 LT and 18:00 – 20:00 LT are most pronounced for all the seasons. At Ougadougou, it is up to 19% during March equinox, and -34% during June solstice at 06:00 LT and 05:00 LT respectively. While at Manila it is up to 18% during December solstice to -12% during March equinox around 04:00 LT and 19:00 LT respectively from Fig. 5 (a) – (d).

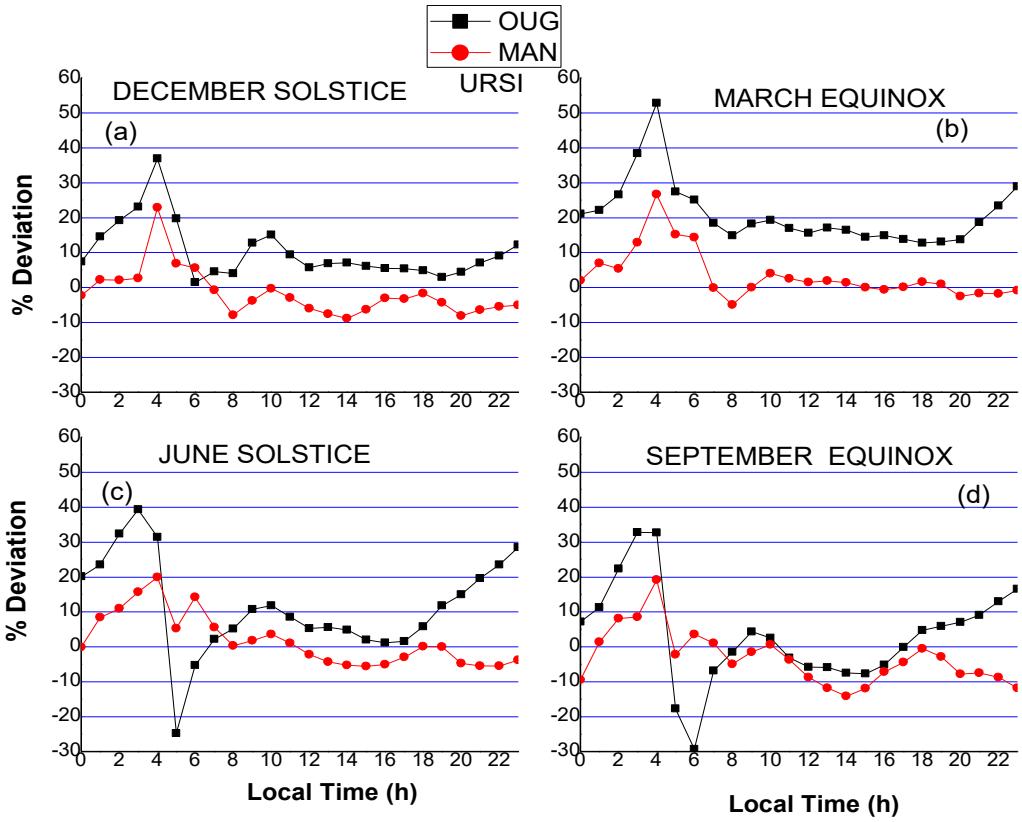

Fig. 6: Percentage deviations of the IRI-2016 model (URSI option) foF2 from the observed foF2 values for all seasons across the entire stations during Minimum Phase of Solar Activity (MnPSA) year, (1986)

From Fig. 6(a) - (d) during M_nPSA year the positive and negative percentage deviations are most pronounced around 04:00 – 08:00 LT and 18:00 – 23:00 LT for all the seasons. At Ougadougou the deviation is up to 52% during March equinox to -30% during September equinox around 04:00 LT and 06:00 LT respectively. While at Manila; it is up to 28% during March equinox to -12% during September equinox around 04:00 LT and 14:00 LT respectively.

3.4 Percentage Deviation of Iri-2016 (CCIR Option) Derived foF2 from The Observed foF2 Values

Fig. 7 - 8 (a) – (d) depicted the percentage deviations of IRI – 2016 model (CCIR option) from the observed foF2 data for all seasons at the two stations during MPSA year (1989) and M_nPSA year (1986) respectively. The CCIR option percentage deviation also exhibits distinct positive and prominent negative deviations between the hours of 00:00 – 08:00 LT and around 19:00 – 23:00 LT just like the URSI option. The deviations between 9:00 – 18:00 LT are fairly close and follow comparable patterns for most of the seasons

except at December solstice in MPSA year and March equinox in MnPSA whose deviation patterns are different from the other seasons.

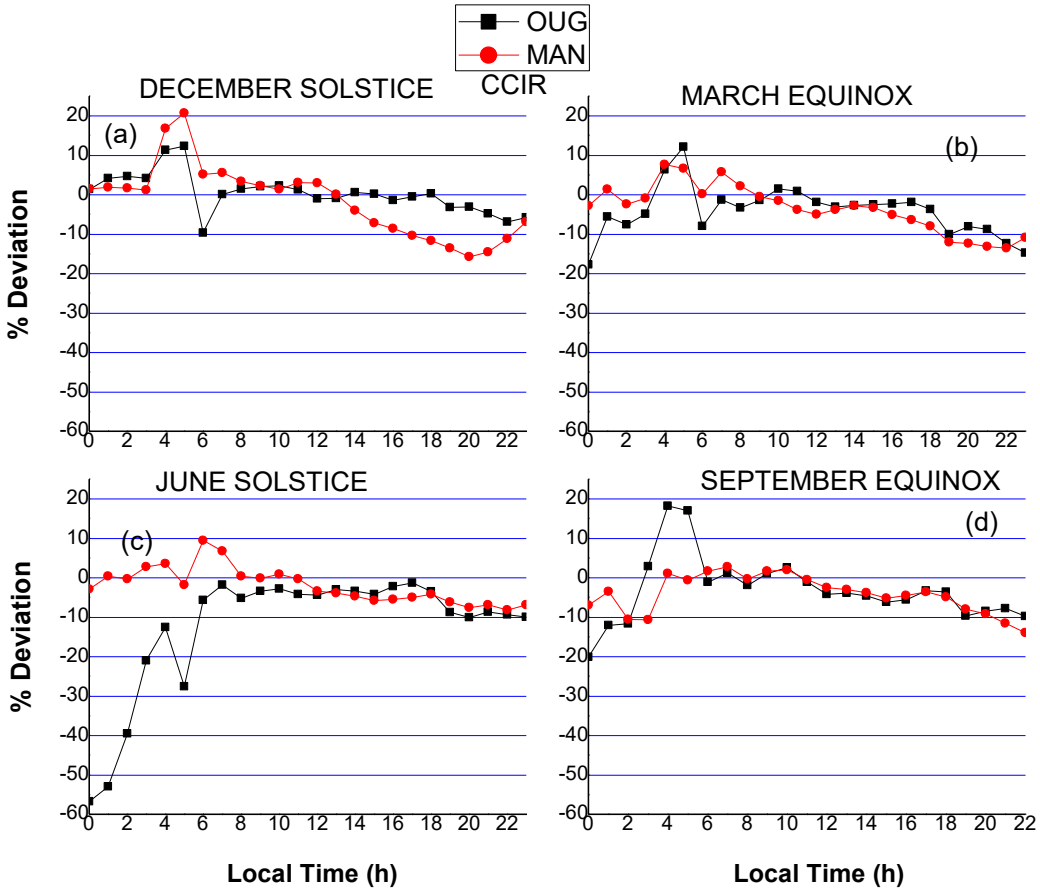

Fig. 7: Percentage deviations of the IRI-2016 model (CCIR option) foF2 from the observed foF2 values for all seasons across the entire stations during Maximum Phase of Solar Activity (MPSA) year, (1989)

During MPSA year, the positive and negative deviations occurring around 04:00 – 07:00 LT and 19:00 – 20:00 LT are noticeable for all the seasons at the two stations. At Ougadougou, the deviation was up to 19% during September equinox and -58% during June solstice around 4:00 LT and 0:00 LT respectively. At Manila, iit is up to 20% during December solstice and -18% during December solstice, around 5:00 LT and 20:00 LT respectively as seen in Fig. 7(a) – (d).

From Fig. 8 (a) – (d), the positive and negative percentage deviations during the MnPSA year are mostly pronounced around 03:00 - 08:00 LT and 14:00 – 23:00 LT for all the seasons. At Ougadougou, it was up to 52% during June solstice and (-18%) during December solstice around 04:00 LT and 06:00 LT respectively. While at Manila, the deviation was up to 30% during December solstice and (-38%) during March equinox, around 3:00 LT and 6:00 LT respectively.

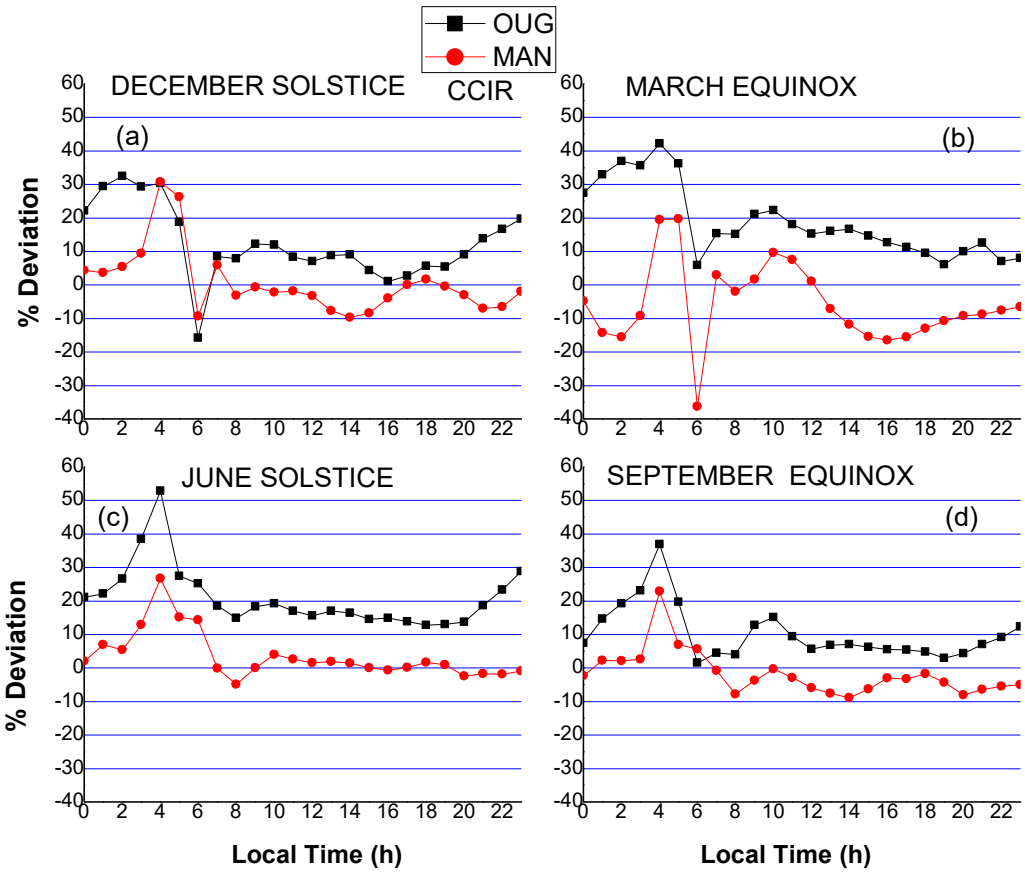

Fig. 8: Percentage deviations of the IRI-2016 (CCIR option) foF2 from the observed foF2 values for all seasons across the entire stations during Minimum Phase of Solar Activity (MnPSA) year, (1986)

Observation from all the percentage deviation figures above at the two stations revealed that the highest positive and negative deviations were observed mostly during the post-midnight hours. This may be attributed to the absence of solar radiation and the gas composition of the O_2/N_2 ratio of the F2-layer which hinders the rate of recombination of ions which the IRI-2016 model cannot correctly predict. [10] explained that the observed night increase in the foF2 variation with decreasing solar activity in terms of low reference value and ion loss is because at night time, the ionospheric electron density is dependent on the recombination rate, which is influenced by the gas compositions and the magnetic meridional winds. Also, [9], reported that the daytime and nighttime disparity is partially due to the lower mean values at night, which for related absolute variability results in a higher deviation percentage at night.

The high percentage deviations observed most especially at Ougadougou in the African sector may be ascribed to lack of availability of large volume data since the predictive ability of a model depends on data availability. [35] reported that the predictive ability of IRI model is strongly dependent on reaching the experimental data at that place where the prediction is made. Secondly, since Ougadougou is located below the equatorial ionisation anomaly EIA crest region, the variation of the observed foF2 is influenced by the electric field in the magnetic equator region. [26] stated similar observation with Guangzhou station located close to the EIA crest region. Generally, the discrepancy in IRI-model data (foF2) as compared to observed foF2 data in equatorial and low latitude region is found to be larger and significant than at mid- latitude region since the equatorial and low latitude region is adversely affected by the E x B forces [44]. In addition,

it is also due to the strong dependence of the equatorial and low latitude ionosphere on the strength of the equatorial electrojet [45, 46, 19] and neutral winds [47, 48, 26]. The IRI-2016 model may not be able to accurately account for the variation of an ionosphere driven by these two factors without discrepancy in numerous physical phenomena, such as the equatorial electrojet, neutral winds, and tidal impacts, have an impact on the equatorial ionosphere. The nonlinear interactions between these processes make it difficult to adequately represent the aggregate impact of these processes in a model [47, 48, 26, 53]. Secondly, due to factors including solar radiation, geomagnetic activity, and seasonal changes, the equatorial ionosphere shows great spatial and temporal variability. In-depth knowledge of the underlying Physics is necessary in order to accurately assess and model this variability [45, 46, 26,43].

Another reason is data availability. Data and observations are used by predictive models to calibrate and validate their output. In the equatorial areas, data availability can be constrained, making it difficult to characterize and forecast ionospheric activity with precision (32 – 33), [35], (50 – 53). Finally, discrepancy occurred as a result of model limitations. Models are based on specific assumptions and parameterizations and are simplifications of the real world. The quality of these hypotheses and parameterizations affects how accurate the forecasts are. The model may have difficulty in predicting changes in the equatorial ionosphere critical frequency if it does not adequately represent the underlying Physics or if its input data are insufficient (32 – 33), (50 – 53). It's vital to note that no model is perfect and that no model can anticipate ionospheric fluctuations with 100% accuracy due to inherent constraints. Ionospheric models like the IRI-2016 model's accuracy is influenced by a number of variables, including the caliber and accessibility of the input data, the complexity of the underlying Physics, and the parameterization and application of the model. (32 – 33), [47, 26, 48].

IRI-model forecasts are most accurate in high and mid-latitudes because of the high number of ionosonde stations. And are less accurate at equatorial and low latitudes where the ionosphere shows very high variable conditions due to lack of wide spread of ionospheric stations [6, 10, 52]. The equatorial ionosphere is a dynamic region with many physical processes combining to cause large fluctuations, making it a particularly difficult location to precisely model. Critical frequencies and other ionospheric parameters can change due to the equatorial ionosphere being affected by variables like solar activity, geomagnetic disturbances, and atmospheric dynamics [35, 32, 26], (49 – 53).

Furthermore, observations from the figures showed that both options of the model performed better in the Asian longitudinal sector than in the African longitudinal sector. This may be ascribed to the following factors;

(a) *Data Availability and Quality*: For setup, calibration, and validation, ionospheric models need precise and complete input data. The performance of the model could be affected by differences in data availability and quality between the Asian and African longitudinal sectors. Predictions may be less accurate if there are fewer or less trustworthy measures available in the African sector (32 – 33), [35], (52 – 53).

(b) *Geomagnetic Activity*: The ionosphere can be greatly impacted by geomagnetic activity, such as magnetic storms or sub-storms. Different longitudinal sectors of these disturbances may exhibit different traits and intensities. The model may not function as well in the African sector if the geomagnetic activity is different or if iits algorithms and parameterizations are more suited to the geomagnetic circumstances common in the Asian sector [47, 48, 26, 53].

(d) *Localized Ionospheric Effects*: It is possible that some ionospheric effects or phenomena are more common in one longitudinal sector than the other. These factors, such as plasma bubbles or the equatorial ionization anomaly (EIA), can significantly affect the ionospheric variability. The algorithms or empirical formulations of the model could not generalize well to the African sector if they are designed for certain ionospheric phenomena in the Asian sector (51 – 53).

(e) *Model Development and Validation*: Extensive investigation and cooperation with regional scientific groups are required for the creation and validation of ionospheric models. The IRI-2016 model may perform better

in the Asian sector compared to the African sector if it has undergone greater refining and validation in that sector, benefiting from a larger body of research and data from that region (32 – 33), [36], (50 – 51).

4. CONCLUSION

The study of the seasonal variation of the F2-layer critical frequency and comparison with the IRI-2016 model during two extremes of solar activity phase of solar cycle 22 was carried out. Data from Ougadougou (Geomagnetic Latitude 0.59 ^{o}N, Geomagnetic Longitude 71.46 ^{o}E) in the African longitudinal sector and Manila (Geomagnetic Latitude 3.4 ^{o}N, Geomagnetic Longitude 191.1 ^{o}E) in the Asian longitudinal sector during MPSA year (1989) and MnPSA year (1986) respectively, were investigated. Seasonal mean values of the IRI-2016 model of both options showed remarkable improvement in predicting the observed foF2 values at these two stations even though the IRI-2016 model underestimates and overestimates the observed foF2 at certain hours/seasons in these stations. The discrepancy (underestimation and overestimation) in the IRI-2016 model is found larger during the MPSA year than during the MnPSA year. The highest positive and negative % deviations were observed mostly during the post-midnight hours. The URSI option performs better than the CCIR option since its predicted values are much closer to the observed values. Both options of the model perform better in the Asian longitudinal sector than in the African longitudinal sector.

ACKNOWLEDGEMENTS

The authors acknowledge the Community Coordinated Modelling Centre (CCMC) IRI (https://ccmc.gsfc.nasa.gov/modelweb/models/iri2016_vitmo.php), and Space Physics Interactive Data Resources (SPIDR) (https://spidr.ngdc.noaa.gov), for providing the predicted foF2 IRI-2016 data and observational foF2 values for the period under consideration in this study.

COMPETING INTERESTS

Authors have declared that no competing interests exist.

AUTHORS' CONTRIBUTIONS

Eugene Onori designed the study, performed the statistical analysis, wrote the protocol, and wrote the first draft of the manuscript. Emmanuel Somoye, Abiola Ogungbe and Ogwala Aghogho managed the analyses of the study. All authors managed the literature searches, read and approved the final manuscript.

REFERENCES

1. Rishbeth H, and Mendillo M. Patterns of F2-layer variability. Journal of Atmospheric and Solar-Terrestrial Physics. 2001; 63 (15). 1661-1680.

2. Rishbeth H. The equatorial F-layer: progress and puzzles. Annales Geophysicae. 2000; 18: 730–739.

3. Fejer BG. Low latitude ionospheric electrodynamics. Space Sci. Rev. 2011; 158 (1): 145 –166.

4. Kouris SS, Fotiadis DN, Xenos TD. On the day-to-day variation of foF2 and M (3000) F2 Advances in Space Research. 1998; 22(6): 873-876.

5. Chattopadhyay R. Covariation of Critical Frequency of F2-layer and relative Sunspot number. Bull Astronomical Society of India. 2000; 28: 657-661.

6. Gulyaeva TL, Mahajan, KK. Dynamic boundaries of the ionosphere variability Advances in Space Research. 2001; 27(1): 91- 94.

7. Kouris SS, Fotiadis DN. Ionospheric variability: a comparative statistical study Advances in Space Research. 2002; 29(6): 977 – 985.

8. Sethi NK, Dabas RS, Singh L, Vohra VK, Veenadhari B, Garg SC. Results of foF2 and Ne-h profiles at low latitude using recent digital ionosonde observations and their comparison with IRI-2000. Journal of Atmospheric and Solar-Terrestrial Physics. 2003; 65 (6): 749-755.
.

9. Bilitza D, Obrou OK, Adeniyi JO, Oladipo O. Variability of foF2 in the equatorial ionosphere. Advances in Space Research. 2004; 34: 1901 - 1906.

10. Chou YT, and Lee CC. Ionospheric variability at Taiwan low latitude station:
Comparison between observations and IRI 2001 model. Advances in Space Research. 2008; 42: 673–681.

11. Akala AO, Seemala GK, Doherty PH, Valladares CE, Carrano CS, Espinoza J, et al. Comparison of equatorial GPS-TEC observations over an African station and an American station during the minimum and ascending phases of solar cycle 24. Annales Geophysicae. 2013; 31: 2085 – 2096. doi:10.5194/angeo-31-2085 - 2013.

12. Akala AO, Adeloye A B, and Somoy EO. Ionospheric foF2 variability over the Southeast Asian sector. *Journal of* Geophysical Research, 2010; 115: 1-7 A09329, doi:10.1029/2010JA015250.

13. Oladipo OA, Adeniyi JO, Radicella SM, Adimula IA. Variability of the ionospheric electron density at fixed heights and validation of IRI- 2007 profile's prediction at Ilorin. Advances in Space Research. 2011; 47: 496 – 505

14. Somoye EO, Akala AO, Adeniji-Adele RA, Iheonu EE, Onori EO, Ogwala A. Equatorial F2 characteristic variability: A review of recent observations. Advances in Space Research. 2013; 52: 1261–1266.

15. Somoye EO, Akala AO, Ogwala A. Day to day variability of h'F and foF2 during some solar cycle epochs. Journal of Atmospheric and Solar-Terrestrial Physics. 2011; 73: 1915 –1922.

16. Prakash K, Purhit PK. Owal AK. Study of ionospheric F2-layer characteristics at low, mid and high latitudes. International Journal of science and Research. 2012; 3: 1509 – 1513.

17. Quattara F. IRI-2007 foF2 Predictions at Ouagadougou Station during Quiet Time Periods from 1985 to 1995. Archives of Physics Research. 2012; 4: 12 – 18.

18. Quattara F, and Amory-Mazaudier C. Statistical study of the equatorial F2-layer critical frequency at Ouagadougou during solar cycles 20, 21, and 22 using Legrand and Simon's classification of geomagnetic activity. Journal of Space Weather Space Climate. 2013; 2(A19): 1- 9. DOI: 10.1051/swsc/2012019.

19. Oyeyemi EO, Adewale AO, Adeloye AB, Olugbon B. An evaluation of the IRI-2007 storm time model at low latitude stations Advancesin Space Research. 2013; 5: 1737 – 1747.

20. Oyeyemi EO. Bolaji S, Adewale AO, Akala AO, Oladipo OA, Olugbon B, et aI. Ionospheric Variations in the F-Region of the Equatorial Ionization Anomaly Crest: Comparison between Observations and IRI-2012 Model Predictions. American Geophysical Union, Fall Meeting 2015; 2015AGUFMSA51A2381O.

21. Atac T, Ozguc A, Petas R. The variability of foF2 in different phases of solar cycle 23. Journal of Atmospheric and Solar-Terrestrial Physics. 2009; 71: 583 – 588 doi: 10.1016/j.jastp.2009.01.004.

22. Adebesin BO. On the ionospheric variability of critical frequency along the equator anomaly trough and plausible role of vertical E × B drift. Journal of Life and Physical Sciences. 2014a; 5(1): 37 – 51.

23. Adebesin BO, Adekoya BJ, Ikubanni SO, Adebiyi SJ, Adebesin OA, Joshua BW, et al. Ionospheric foF2 morphology and response of F2 layer height over Jicamarca during different solar epochs and comparison with IRI-2012 model; J. Earth Syst. Sci. 2014b; 123(4): 751–765.

24. Adebesin BO, Rabiu AB, Obrou OK, Adeniy JO. Ionospheric peak electron density and performance evaluation of IRI-CCIR near magnetic equator in Africa during two extreme solar activities. Space Weather. 2018; 16: 230 – 244. https://doi.org/10.1002/ 2017SW001729.

25. Atiq M, Ameen MA, and Sadiq N. The Study of GPS TEC and its Comparison with IRI-2016 and NeQuick2 Predictions at Sonmiani during High Solar Activity Period of Solar Cycle 24. Journal of Space Exploration, 2018; 7(3): 1 – 15.

26. Rao SS, Chakraborty M, Pandey R. Ionospheric variations over Chinese EIA region using foF2 and comparison with IRI-2016 model. Advances in Space Research. 2018; 62:84 – 93.

27. Ogwala A, Onori E, Ogabi C, Ometan O, Kayode Y, Adeniji-Adele R, et al. Variations in the Maximum Electron Density of the F2 Layer (NmF2) over the Middle Latitude Station of Grahamstown, South Africa, during Solar Cycle 23. Adv Environ Eng Res. 2022; 3(4): 1-16. doi:10.21926/aeer.2204048.

28. Ogwala A, Somoye OE, Sampad K P, Ogunmodimu O, Onori E, Sunil KS, et al. Total Electron Content at Equatorial and Low-, Middle- and High-Latitudes in African Longitude Sector and Its Comparison With IRI-2016 And IRI-PLAS 2017 Models. Advances in Space Research. 2021; 68: 2160 - 2176 https://doi.org/10.1016/j.asr.2020.07.013

29. Ogwala A, Somoye EO, Ogunmodimu O, Adeniji-Adele RA, Onor EO, et al. Diurnal, seasonal and solar cycle variation in total electron content and comparison with IRI-2016 model at Birnin Kebbi. Annales Geophysicae. 2019; 37: 775 - 789.

30. Onori EO, Somoye EO, Ogwala A. Study of the Relative Variability of F2-Layer Critical Frequency at Three Different Longitudinal Sectors in the Equatorial Ionosphere. Applied Physics. 2020; 3(1): 1-16. DOI: https://doi.org/10.31058/j.ap.2020.32001.

31. CCIR. CCIR.International Telecommunication Union, Geneva. 1991.

32. Bilitza D, Altadill D, Truhlik V, Shubin V, Galkin I, Reinisch B, et al. International Reference Ionosphere 2016: From ionospheric climate to real-time weather predictions. Space Weather. 2017; 15: 418 – 429, doi:10.1002/2016SW001593

33. Bilitza D, Altadill D, Reinisch B, Galkin I, Shubin V, Truhlik V. The international reference ionosphere: model update 2016. Geophysical Research Abstract. 2016; 18: 9671.

34. Bilitza D, and Reinisch BW. International reference ionosphere 2007: improvements and new parameters. Advances in Space Research. 2008; 42: 599–610.

35. Bilitza D, David A, Yongliang Z, Chris M, Vladimir T, Phil R, et al. The International Reference Ionosphere 2012 – a model of international collaboration. Journal Space Weather Space Climate. 2014; 4 A07.
[36] Bilitza D, Mckinnell L, Reinisch B, Fuller-Rowell T. The international reference ionosphere today and in the future. Journal of Geodetics. 2011; 85: 909 – 920.

37. Ezquer RG., Mosert M, Corbella R, Erazu M, Radicella SM., Cabrera M, et al. Day-to-day variability of ionospheric characteristics in the American sector. Advances in Space Research. 2004; 34: 1887–1893.doi: 10.1016/j.asr.2004.03.016.

38. Ezquer RG, Ortiz de Adler N, Radicella SM, Mosert de Gonzalez M, and Manzano JR. IRI and BPM total electron content predictions for Tucuman. Advances in Space Research.1995; 15: 121–124.
[39] Faynot JM, and villa P. F-Region at the Magnetic Equator. Annals of Geophysics.1979: 35: 1- 9.

40. Gnabahou DA, Ouattara F, Nanéma E, Zougmoré F. foF2 Diurnal Variability at African Equatorial Stations: Dip Equator Secular Displacement Effect. International Journal of Geosciences. 2013; 4: 1145 – 1150..

41. Bolaji OS, EO. Oyeyemi, OE. Jimoh, A Fujimoto, PH Doherty, OP Owolabi, et al. Morphology of the equatorial ionization anomaly in Africa and Middle East due to a sudden stratospheric warming event. Journal of Atmospheric and Solar-Terrestrial Physics. 2019; 184: 37-56. https://doi.org/10.1016/j.jastp.2019.01.006

42. Zolesi B, and Cander LR. Ionospheric Prediction and Forecasting. Springer Geophysics. 2014; DOI: 10.1007/978-3-642-38430-1_2, © Springer-Verlag Berlin Heidelberg.

43. Rabiu AB, Onwumechili CA, Nagarajan N, and Yumoto K. Characteristics of equatorial electrojet over India determined from a thick current shell model. Journal of Atmospheric and Solar-Terrestrial Physics. 2013; 92: 105–115.

44. Kumar S, Eng LT. and Dhimas SM. Impacts of solar activity on performance of the IRI-2012 model predictions from low to mid-latitudes. Earth, Planet and Space. 2015; 67(42): 1 – 17, DOI: 10.1186/s40623-015-0205-3.

45. Dabas RS, Bhuyan PK, Tyagi TR, Bhardwaj RK. Day-today changes in ionospheric electron content at low latitudes. Radio Science. 1984; 19 (3); 749–756. https://doi.org/10.1029/RS019i003p00749.

46. Chandra H, Sharma S, Aung SW. Day to day variability in the critical frequency of F2-layer over the anomaly crest region. Ahmedabad. Journal of Industrial Geophysical Union. 2009; 13 (4): 217 – 226.

47. Heelis RA, Coley WR, Burrell AG, Hairston MR, Earle GD, Perdue MD, et al. Behaviour of the O+/H+ transition height during the extreme solar minimum of 2008. Geophysical Research Letters. 2009; 36 (A02303): doi: 10.1029/2009GL038652.

48. Stening RJ, Meek CE, Manson H. Upper atmosphere wind systems during reverse equatorial electrojet events. Geophysical Research Letter. 1996; 23: 3243 doi:10.1029/96GL02611

49. Akala AO, Somoye EO, Adewale AO, Ojutalayo EW, Karia SP, Idolor RO, et al. Comparison of GPS-TEC observations over Addis Ababa with IRI-2012 model predictions during 2010–2013. Advances in Space Research. 2015; *56*(8), 1686–1698. https://doi.org/ 10.1016/j.asr.2010.01.003

50. Tariku YA. Comparison of performance of the IRI 2016, IRI-Plas 2017, and NeQuick 2 models during different solar activity (2013–2018) years over South American sector. Radio Science. 2020; *55*, e2019RS007047. https://doi.org/10.1029/2019RS007047

51. Tsagouri I, Goncharenko L, Shim JS, Belehaki A, Buresova D, & Kuznetsova MM. Assessment of current capabilities in modeling the ionospheric climatology for space weather applications: foF2 and hmF2. Space Weather. 2018; 16, 1930–1945. https://doi.org/ 10.1029/2018SW002035

52. Chen J, Ren X, Zhang X, Zhang J, & Huang L. Assessment and validation of three ionospheric models (IRI-2016, NeQuick2, and IGS-GIM) from 2002 to 2018. *Space Weather*. 2020; *18*, e2019SW002422. https://doi.org/10.1029/2019SW002422

53. Adebiyi SJ, Adimula IA, Oladipo OA, Joshua BW. Assessment of IRI and IRI-Plas models over the African equatorial and low-latitude region. Journal of Geophysical Research: Space Physics. 2016; *121*, 7287–7300. https://doi.org/10.1002/2016JA022697